Fermi National Accelerator Laboratory

TM-1434
2500.000

Sources for Proportional Tube Gain Variation - What to Do About It*

Y. Fukui, M. Mishina
KEK

Y. Hayashide, S. Kanda, S. Kim, K. Kondo, M. Masuzawa,
S. Miyashita, H. Miyata, S. Mori, Y. Morita,
T. Ozaki, M. Shibata, K. Takikawa
University of Tsukuba

Y. Muraki
Institute for Cosmic Ray Research, Tokyo University

October 1985

*Presented at (and appearing in the Proceedings of) the Gas Sampling Calorimetry Workshop II, Fermilab, Batavia, Illinois, October 31 - November 1, 1985

SOURCES FOR PROPORTIONAL TUBE GAIN VARIATION

WHAT TO DO ABOUT IT

Y. Fukui, M. Mishina

KEK

Y. Hayashide, S. Kanda, S. Kim, K. Kondo, M. Masuzawa,

S. Miyashita, H. Miyata, S. Mori, Y. Morita,

T. Ozaki, M. Shibata, K. Takikawa

University of Tsukuba

Y. Muraki

Institute for Cosmic Ray Research, Tokyo University

Abstract

In the high-energy domain systematic uncertainties become a substantial fraction of attainable energy resolution of a proportional tube electromagnetic calorimeter. Sources of nonuniformity and fluctuation of calorimeter response are discussed and test data on the magnitude of the effects are presented. Possible ways of maintaining these effects under control are discussed and test data are discussed which demonstrated that such effects could in fact be monitored and corrected to less than 1%.

Introduction

Different from cases in which proportional chambers are used for track measurement, gain nonuniformity and gain variation in time are crucial issues for gas calorimeters. Especially for electromagnetic calorimeters designed for a high-energy environment beyond a few tens of GeV, it becomes important because the intrinsic energy resolution diminishes to several percent, or even reaches to a few percent in higher energies. It has been empirically known 1) that the following formula for energy resolution holds well for most proportional tube electromagnetic calorimeters;

$$\sigma/E = 30\% \sqrt{t/E}$$

where t is the sampling thickness in radiation length.

In most cases, lead absorber panels are 2 to 5 mm thick and when putting such numbers into the above formula, one obtains the energy resolutions shown in Table I for various energies.

Especially in high-energy p-p or $\bar{p}$-p colliders like CDF at Fermilab, and especially in the forward angles, the energy range to be covered is quite large. If we take transverse momentum P_T as a meaningful parameter corresponding to mass scale of observable particles, we see that seemingly high linear momentum is within a range of not very high P_T.

In such high energy range the systematic uncertainties become significant fractions of the final energy resolution.

There are many sources for gain variation of proportional chambers, as listed below:

1) Mechanical Structure — Tube Cell Size
   Wire Diameter
   Wire Displacement
2) High Voltage

3) Gas Condition	Temperature	
	Pressure	
	Gas Composition	Gas Composition
		Air Leak
		Outgas

4) Electronics

We discuss what the effects are and present some test data in order to provide a quantitative basis for the discussion.

Test Data on the Effects

1) Mechanical Structure

Irregularity in the mechanical structure is in principle determined at the time of constructon and introduces nonuniformity of the gain having not much to do with gain fluctuation in time. However, in any circumstance, a physics event is evaluated on the basis of certain statistics, in which local nonuniformity has the same effect on the energy resolution as the gain fluctuation in time. Therefore the mechanical structure has to be dealt with with the same degree of care as the time-wise fluctuation.

a) Tube Cell Size: Tubes or multi-cell comb structures are usually made by extrusion out of plastics or metal material. In either case fairly good precision is attained by controlling the conditions of the extrusion process, such as temperature, speed of extrusion, and cooling process. In case of conductive plastic tubes, 7 mm × 7 mm ID was kept to ± 150 μm. A preliminary data indicates that it still corresponds to ±4 to ±5 percent change in the gain.

b) Wire Diameter: There are two sets of data on this effect, one by M. Atac 2) shown in Fig. 1 and another by us shown in Fig. 2. In Fig. 1 the gain is plotted logarithmically against various wire diameters. This was measured on a 2 cm × 2 cm tube. This is not a direct plot of the data, but data at different high voltage points were normalized assuming that there is a gain change by a factor of 2.4 to 2.5 for 100 V voltage change. This assumption is valid for 7 mm to 1.2 cm tubes as is seen later. Locally the trend can be described by a straight line

$$\log G = a D + b,$$

where G is the gain and D is the wire diameter; a and b are constants. This formula can be converted into the following;

$$G_{D1}/G_{D2} = 10^{a(D1-D2)}$$

Taking 25 μm to 75 μm points, the gain change is a factor of 4 for 25 μm diameter change. The formula can be reduced to a case of $\Delta d = 0.5$ μm

$$(G1/G2)_{\Delta\, d=0.5\,\mu m} = (2.4)^{4\ 1/50} = 1.072.$$

This means that 1% change in the anode wire diameter results in 7% gain change.

Fig. 2 shows logarithm of the gain corresponding to 30, 50, and 70 μm diameter wires for 7 mm × 7 mm ID tube. When fitting these with a straight line and then manipulating it in the same way as the previous data, we obtain a factor of 63.1 in the gain for 40 μm diameter change. Then 1% change in diameter corresponds to

$$(G1/G2)_{\Delta\, d=0.5\,\mu m} = (63.1)^{0.5/40} = 1.053,$$

or 5.3% gain change.

c) Wire Displacement: If an anode wire is displaced from the center of a tube, the field will be distorted and the gain will change. In common practice, the wire is supported at the center of a tube at both ends of the tube by precisely shaped wire supports. However, it is not necessarily easy to keep the tube straight, while the wire will be straight with applying an appropriate tension. There are two sets of data shown in Fig. 3. One was measured on a 6.3 mm × 11.3 mm ID rectangular tube and the other was measured on a 7 mm × 10 mm ID rectangular 3) tube. The anode wire was displaced in the direction of a narrower gap in either case. The gain increased with increasing the displacement and the gain change is well described by

$$G_d/G_0 = a(d/D)^b.$$

The relative gain change is proportional to b-th power of d/D, the displacement d normalized by the gap height D, with the constant b of 2.6 to 2.8. It means that if we maintain the straightness of the tube within + 250 μm, the gain variation is less than 1%. Fig. 4 shows another set of data measured on a 7 mm × 7 mm square tube. The exponent b for this data set is about 2.3, similar to the previous data. Interesting to notice is that the effect of the wire displacement is slightly less prominent for the square tube than for the rectangular tube. This is what one can naturally expect because the field strength around the wire is equally shaped by the horizontal and the vertical walls in the square tube whereas in the rectangular tube the walls with a narrower gap have larger effect in shaping the field around the wire which is directly affected by displacing the wire along the normal line to these walls.

2) High Voltage

In the proportional region the dependence of the gain on operating high voltage is well described by a linear dependence in log (Gain) vs. high voltage plot as seen in Figs. 5 and 6. In Fig. 5, the data are on 7 mm × 7 mm ID tubes with 50 μm wire and the gas was Ar - ethane 50% - 50% mixture with 1.4% of ethyl alcohol admixture. 20 to 200 GeV electron beams were injected into the CDF end plug electromagnetic calorimeter and the data points represent the total charge collected from the anode wires plotted logarithmically against the operating high voltage. The linear dependence in this plot leads us to the following formula

$$\log G = a V + b$$

which means the ratio of the gains for two different voltages is proportional to a power of a constant with the voltage difference of the two points as the exponent,

$$G1/G2 = (\text{const})^{V}.$$

From the lines in the graph we read a factor of 2.4 increase in the gain for 100 V increase in the high voltage. Reducing this number to a 1 V increment, we obtain

$$(G1/G2)_{\Delta V=1\ V} = (2.4\sim2.5)^{1/100} = 1.0088.$$

Therefore a 1 V increment results in 0.9% increase in the gain.

In Fig. 6 a preliminary test result on a MAC calorimeter prototype module 4) is plotted. The tube ID was 1.27 cm square. The gas is the same as the previous data but the gas is pressurized to 3 PSIG. The graph reads a factor of 2.2 gain change for 100 V voltage change which reduces to 0.8% gain change for 1 V voltage increment quite similarly to the previous data.

3) Gas Condition

Proportional chamber gain is a function of temperature, pressure, and gas composition.

a) Temperature: Fig. 7 is a log-log plot of the gain of 7 mm × 7 mm ID tube vs. the gas temperature in K° between 0°C and 20°C. For simplicity, we take the trend as a linear dependence. Then the appropriate formula is

$$\ln G = a \ln T + b,$$

which implies

$$G1/G2 = (T1/T2)^a$$

with a = 6.7. Then the gain change for 1°C temperature change around room temperature will be

$$(G1/G2)_{\Delta T=1\,^0C} = (294/293)^{6.7} = 1.023.$$

This is already a significant number.

b) Pressure: A log-log plot of the pressure dependence of the gain of the same tube as the previous one is shown in Fig. 8. The pressure range is between 1000 m bar to 1040 m bar. The relationship is linear and can be formulated in the same manner as the previous data except that the exponent is now negative,

$$(G1/G2) = (P1/P2)^{-a}$$

with a = 7.7. This means that 1% change in the pressure results in 8% change in the gain.

Notice that the exponent is close to the exponent for the previous formula of temperature dependence with reversed sign. Taking into account a possible error, this observation is consistent with the fact that the gain is dependent on the density of the gas. This was observed before on one of our prototype calorimeter modules which was sealed off for eight hours and the signal from 40 GeV electrons did not change within an accuracy of 0.5%.

c) Gas Composition: There is a measurement done by M. Atac 5) for Ar-ethane mixture around 50% - 50% mixing ratio. Two sets of data, one for 25 μm wire and another for 50 μm wire on a 19 mm × 19 mm ID square tube, are in Fig. 9. The gains are plotted logarithmically against the high voltages. We read a change of the gain by about 20% between two data sets for about 2% different, out of 50%, ethane composition. Since it does not seem to be easy to regulate the gas composition much better than 1% level, batch to batch fluctuation of the gain could be significant.

What to Do About It

1) Mechanical Structure

We have seen that the effect of the irregularity in the mechanical structure is amplified in the gain of a proportional tube in terms of percentage. Therefore at the time of the fabrication of chambers it is important to try hard to minimize the nonuniformity of those parameters.

How well can we control these parameters?

As has been discussed, the cell size could be maintained to a tolerance of ±150 μm which is 1.4% for a tube of 7 mm × 7 mm ID. This is still large enough to introduce a few to several percent nonuniformity in the gain. The uniformity of the anode wire diameter is determined by the manufacturer of the wire and we have not much control over it other than specifying at the time of the order. Some companies accept a specification of the tolerance to 0.5% in weight for gold plated tungsten wire that is 0.25% in diameter. Using the formula derived before, if there is 0.25% variation in diameter, we expect

$$(1.05\sim1.07)^{1/4} = 1.013\sim1.017,$$

or 1.3 to 1.7% variation in the gain. The tolerance, according to the company, is meant to be the tolerance of the diameter of the bore of the die, and taking samples in the course of the extrusion the die will be replaced whenever the bore is worn out beyond the tolerance. Therefore even within the tolerance the variation will be further quite gradual and monotone. As far as the same portion of a large batch is used the effect must be in a minute level.

The tolerance of the positioning of the anode wire at the center of the tubes or cells essentially depends on how straight the tubes or cells are within the chamber plane and in perpendicular direction to the plane.

After all the effort to regulate the nonuniformity, it is probably still difficult to suppress the spot to spot nonuniformity down to better than a few percent level. However the response of a calorimeter to an electromagnetic shower is given by the integration of the responses of individual layers and, since the response of individual layer is at most only several percent of the total, layer to layer variation of the response only creates a secondary effect due to a minor fluctuation of the shower depth. Spot to spot variation in the response in any layer of the stack will be also smeared by the integration over the depth and also over the lateral spread of the shower. For this reason one can make a spot by spot calibration map by injecting an electron beam of appropriate energy. Due to the finite lateral profile of the shower, and furthermore in case of cathode readout, due to inherent spread of the induced signal, the mesh of the calibration points can be reasonably coarse. Our experience is that calibrating the entire surface by a 100 GeV electron beam with a mesh as coarse as 3 cm, we could obtain a uniformity of better than $\pm 1\%$ after the correction.

2) High Voltage

Today, commonly used high voltage power supplies are regulated to better than 0.1 V. However, usually the setability, or in other words the reproducibility, is somewhat coarser. Voltage drop across protection resistors due to standing noise current must be kept under control. In our calorimeter modules, 34 quadrant chambers drew 5 to 10 μA dc current which gives rise to 0.5 to 1 V across 10 k Ohm resistor. Instantaneous voltage drop due to a splash of beam-originated particles must be watched, also.

On the other hand, as far as it is stable, a different setting of high voltage simply implies a multiplicable factor well determined to a good accuracy. Therefore a very minimum exercise is to monitor the voltage by a good digital voltmeter and correct the gain for the voltage difference.

3) Gas Condition

Variation of gas condition has a different effect on the gas gain from the effect of the nonuniformity of the chamber and normally it introduces fluctuation in time.

Also due to that, the change in gas composition results in a sizable change in the gain; it does not seem easy to regulate the gas condition to a level of what we would like to achieve.

If one can seal off the calorimeter system with a gas-tight vessel, it probably guarantees the stability of the system until minor air leaks or outgassing changes the gain beyond the tolerance. Even in such a case local temperature nonuniformity must be regulated. Furthermore once the vessel is refilled, the gain may shift unless the refilled gas has exactly the same gas gain as before. If it needs a continuous gas flow to compensate air leak or outgassing, then the condition fluctuates together with the surrounding atmo-

sphere unless a sophisticated gas regulation scheme is implemented. Even if the temperature is regulated to ± 1°C, as has been seen in the data, the gain fluctuates by ± 2.3%. If the gas pressure floats with the barometric pressure quite possibly by ± 5%, the gain change is as large as ± 46%.

Gas composition could be regulated to 0.5% by a well designed system. Still it gives rise to ± 5% level fluctuation in the gain. The effect of air leak into the system and outgassing may not be easy to measure.

After all, except for a case in which the calorimeter is completely sealed off permanently, it is almost impossible to regulate the gas condition or to correct the gain for individual parameter variation to a desirable level in high energy application. Then what can be done after trying hard to regulate the condition is to monitor the overall gain and correct the experimental data for the observed gain variation.

Monitoring of Gas Gain

1) If There is a Momentum Measuring Device in Front

If there is a momentum measuring device in front of the calorimeter, then the calorimeter could be continuously calibrated in situ. However there are several questions to be asked. Abundance of appropriate clean signals, especially electrons, is not always fulfilled. There must be enough numbers of events and then they have to be accepted in the particular trigger for the experiment. Otherwise one frequently needs a special run partially or totally dedicated for the calibration to trace the gain drift in time.

2) If There is No Good Momentum Tagging

If there is no good momentum tagging system in front of the calorimeter, there could be two possible ways of monitoring the gas gain.

a) Monitoring by Minimum Ionizing Particle Signals: One is to use minimum ionizing particle, m.i.p. henceforth, signals. For an electromagnetic calorimeter, m.i.p.'s could be non-interacting hadrons in addition to muons. There are pros and cons. Most likely the usable surface of the calorimeter is entirely exposed to such signals and therefore, even if there is a mild variation in the local gas gain it could be calibrated if there is enough local rate. There are serious drawbacks which have to be cautiously taken into account. M.i.p.'s induce equal magnitude signals from all of the calorimeter layers whereas the electromagnetic shower is dominantly from the layers around shower maximum. Therefore depth-integrated signals may need certain translation to derive the calorimeter response if the gas condition has depth dependent variation. Since m.i.p. signals have broad Landau distribution, one needs to accumulate a fair number of events before one can determine the peak position. If the calibration is to be done simultaneously with the data taking - most likely it is in order not to interrupt the main data taking still, in order to accumulate enough number of events - the rate of recording m.i.p.'s by the specific trigger for the experiment may be a serious limitation. An equally serious problem with m.i.p. signals is the relativistic rise, up to 40%, which is specific to gas sampling. It has to be corrected knowing local momentum distribution with the specific type of trigger for the data taking. Also if the data is collected through the main data acquisition system, it requires large dynamic range for the amplifier-ADC system even though it is possible to use nonlinear or bilinear type ADC. Considering all of these, we conclude that m.i.p. signal could be a useful source for secondary calibration but is not suitable for precision calibration. It will be useful as a means to check overall throughput.

b) Monitoring by Radioactive Source 6) : There is a choice of radioactive source depending on the cell dimensions. An X-ray source is preferable because it penetrates the wall well and makes mono-energetic peak by photoelectric conversion within the gas volume. The energy has to be high enough not to be attenuated too much by the wall and also to obtain noise free peak, but not too high in order to absorb most of the energy of the secondary electrons within the gas volume.

Besides commonly used sources, 5.9 keV X-ray from Fe-55 or 22 keV X-ray from Cd-109, there is a possibility to tune the energy finely by selecting a K X-ray emitting target element bombarded by another primary radiation, which is preferably α-source not to leak it directy. Examples 7) are

Cu	8.04 keV	Sn	25.3 keV
Rb	13.37 keV	Ba	32.06 keV
Mo	17.44 keV	Sm	40.1 keV
Ag	22.10 keV	Tb	44.23 keV

In our case, 5.9 keV X-ray from Fe-55 is adequate for 7 mm × 7 mm plastic tube with 0.8 mm thick wall. The range of the photoconverted 5.9 keV electrons is less than a millimeter. The source could be mounted on the outside of the tube and make a reasonably sharp peak, 10% in fwhm. On the other hand, 22-keV X-ray from Cd-109 cannot make a decent peak because the range of 22 keV electrons is over a centimeter in atmospheric pressure Ar-ethane mixture.

If we monitor a peak of such X-rays flowing the same gas as the calorimeter, the peak position must exactly reflect the gain variation due to the gas condition fluctuation. It is desirable to use a tube identical in dimension to the tubes in the calorimeter. Then the gain correspondence between the monitoring tube and the calorimeter is one to one.

Ideally the sources can be mounted directly onto the tubes of the calorimeter itself. Then there is no correction to be made for the difference in the gas condition. Furthermore if a number of sources are distributed in the calorimeter, the source signals will represent the local gas conditions if there is any local variation. Since the signal is so small compared to the shower induced signal - about 30 MeV electron induced shower equivalent - it does not disturb the main beam associated shower signals. Also the source signals have to be read out by their own trigger. As far as the source is weak enough, chance coincidence of the source signal to be read off by the main beam trigger will be rare.

Since the source signals are from local spots on individual tubes it is preferable to pick them up individually but not from ganged bus lines. In many cases main signal is from cathode pads or strips to form a projected tower geometry. In such cases, accuracy of the energy measurement is required for these signals and the signals from the anode wires are for secondary supplemental informations and can be manipulated to pick off the monitoring source signals independently from the main beam-triggered data stream. Thus the source signals can be treated in a special way to preamplify the small signals without requiring large dynamic range for the main data taking electronics.

For a large detector system, the trigger rate is limited by the speed of magnetic tape to write large amount of data. If the monitoring source signals are read out independently from the main data stream, then one can trigger the read out system with fairly high rate so that enough statistics are accumulated within a short period to be able to track the gain variation in time to a good accuracy in a continuous manner.

For a Gaussian distribution, the accuracy of the peak determination is given by a formula

$$\sigma_{peak}/E_{peak} = (1/\sqrt{n})\ \sigma/E$$

where n is the number of events under the peak. If we use 10% as the intrinsic resolution σ/E for 5.9 keV peak of Fe-55, then 10^4 events give 0.1% accuracy. Since the time constant of the gas condition change is something like 10 min, 10^4 events only means 17 Hz.

Test Results of Monitoring by Radioactive Source

We have tested the idea of monitoring gas gain of a calorimeter by embedded radioactive sources. We embedded six Fe-55 sources in a gas vessel for a quadrant module of the final CDF end plug electromagnetic calorimeter. Each source was a 50 μm wire with Fe-55 deposited on the surface over a length of 2 cm. It was mounted on the outside surface of a short - about 10 cm long - conductive plastic tube which is identical to those used in the calorimeter. These tubes were distributed around the outer circumference of the module within the vessel. Signals were read out independently from the calorimeter signal by self triggering and signals were amplified before being fed into LeCroy 2285A ADC's.

The test was continued for four weeks within which for the first two weeks the module was tested by high energy electron beam. In the course of the test, 100 GeV electons were injected from time to time into a fixed reference point of the module. In Fig. 10 the observed pulse heights of 100 GeV electrons and the peak position of the monitoring sources averaged over six sources are plotted in time sequence. The r.m.s. variation in this period of the peak positions of the tubes No. 2 through No. 6 normalized by No. 1 are listed in Table 2. As is seen in this table the r.m.s. fluctuation is much

less than 1% for any of the tubes. That means all of the tubes are tracking each other quite precisely. It should be noted that these results are obtained without any correction for the electronics response. Furthermore it is seen in the figure that the average peak position is tracing the fluctuation of the 100 GeV electron signals in the first two weeks. The r.m.s. fluctuation of the ratio of these two values in this period was 0.75%. This demonstrates that monitoring the calorimeter gas gain by embedded radioactive sources is in fact an accurate and workable solution. Also it indicates that today there are commercially available electronics stable enough to maintain this level of accuracy for long term.

Conclusions

1) Approaching to high energy domain, intrinsic energy resolution reaches to several to a few percent level. Then systematic error becomes non-negligible.
2) Many parameters affect the gain of the calorimeter significantly.
3) It is possible to correct nonuniformity of a calorimeter to better than 1% by point-by-point beam calibration.
4) It has been demonstrated that the gain fluctuation in time could be well monitored by embedded radioactive sources to an accuracy of better than 1%.

Acknowledgement

We express our sincere thanks to M. Atac for letting us use his data for this talk. We also owe him much for many useful discussions throughout the work and reading the manuscript. The work was supported in part by the U.S. Department of Energy and in part by the Japanese Ministry of Education, Science and Culture.

References

1) M. Atac, IEEE Transactions **NS-28**, 492 (1981).
2) M. Atac, Private communication.
3) Y. Fukui and Y. Hayashide, Fermilab CDF Note 267.
4) M. Atac et al., Private communication.
5) M. Atac, Private communication.
6) Originally suggested by M. Atac.
7) Amersham Corporation Catalogue.

Table Captions

Table 1: Expected energy resolution of proportional tube electromagnetic calorimeter.

Table 2: R.m.s. fluctuation, in four week period, of peak positions of 5.9 keV X-rays from Fe-55 observed with embedded monitoring proportional tubes. The peak positions of tubes No. 2 through No. 6 are normalized by the peak position of tube No. 1.

Figure Captions

Fig. 1: A logarithmic plot of proportional tube gain for various anode wire diameters. The tube was 2 cm × 2 cm in ID. Data measured by M. Atac 2) at different high voltages were translated assuming a factor of 2.4 to 2.5 gain change for 100 V high voltage change.

Fig. 2: A logarithmic plot of proportional tube gain for different anode wire diameters. The tube ID was 7 mm × 7 mm.

Fig. 3: Effect of displacement of an anode wire from the center of a proportional tube. Two sets of data were taken, one on a tube with 7 mm × 10 mm ID and another with 6.3 mm × 11.3 mm ID. In both cases the anode wires were 50 μm in diameter.

Fig. 4: Effect of anode wire displacement for 7 mm × 7 mm ID square tube with 50 μm anode wire 3).

Fig. 5: Logarithmic plot of wire gain against high voltage. High energy electron beams of 20 to 200 GeV were injected into a CDF end plug calorimeter module which consisted of 34 layers of 7 mm × 7 mm proportional tube panels interleaved with 2.7 mm lead sheets. Anode wires are 50 μm in diameter.

Fig. 6: A logarithmic plot of wire gain against high voltage on MAC electromagnetic calorimeter prototype 4). Ar-ethane mixture was pressurized to 3 PSIG.

Fig. 7: A log-log plot of wire gain vs. temperature measured on a 7 mm × 7 mm ID square tube with 50 μm anode wire. Ar-ethane mixture was used.

Fig. 8: A log-log plot of wire gain vs. pressure measured on the same tube as for Fig. 7.

Fig. 9: Effect of gas composition change measured by M. Atac 5). Gain is plotted logarithmically against high voltage for 25 μm wire and 50 μm wire with the gas composition as the parameters.

Fig. 10: Pulse height of 100 GeV electrons observed on a quadrant module of CDF end plug electromagnetic calorimeter and peak positions of 5.9 keV X-rays from Fe-55 averaged over six monitoring tubes.

Table 1

Expected Energy Resolution of Proportional Tube Electromagnetic Calorimeter

Empirically; $\sigma/E = 30\% \sqrt{t/E}$
$t = 2 \sim 5$ mm
$= 0.36 \sim 0.89$ radiation length
$\sigma/E = (17.9 \sim 28.3)\ \% / \sqrt{E}$

$\theta = 5°$	$10°$	$30°$		
$\eta = 3.13$	2.44	1.32		t = 2 mm~5 mm
	P		E	σ/E
1.7 GeV	3.5 GeV	10 GeV	20 GeV	4.0~6.3%
4.4	8.7	25	50	2.5~4.0
8.7	17.4	50	100	1.8~2.8
17.4	34.7	100	200	1.3~2.0
43.5	86.8	250	500	0.8~1.3

Table 2

R.m.s. Fluctuation of Normalized Height of 5.9 keV Peak of Fe-55 Observed on Monitoring Tubes in Four Week Period

Monitoring Tube No. 2 / Monitoring Tube No. 1	+0.54%
Monitoring Tube No. 3 / Monitoring Tube No. 1	+0.47%
Monitoring Tube No. 4 / Monitoring Tube No. 1	+0.27%
Monitoring Tube No. 5 / Monitoring Tube No. 1	+0.50%
Monitoring Tube No. 6 / Monitoring Tube No. 1	+0.70%

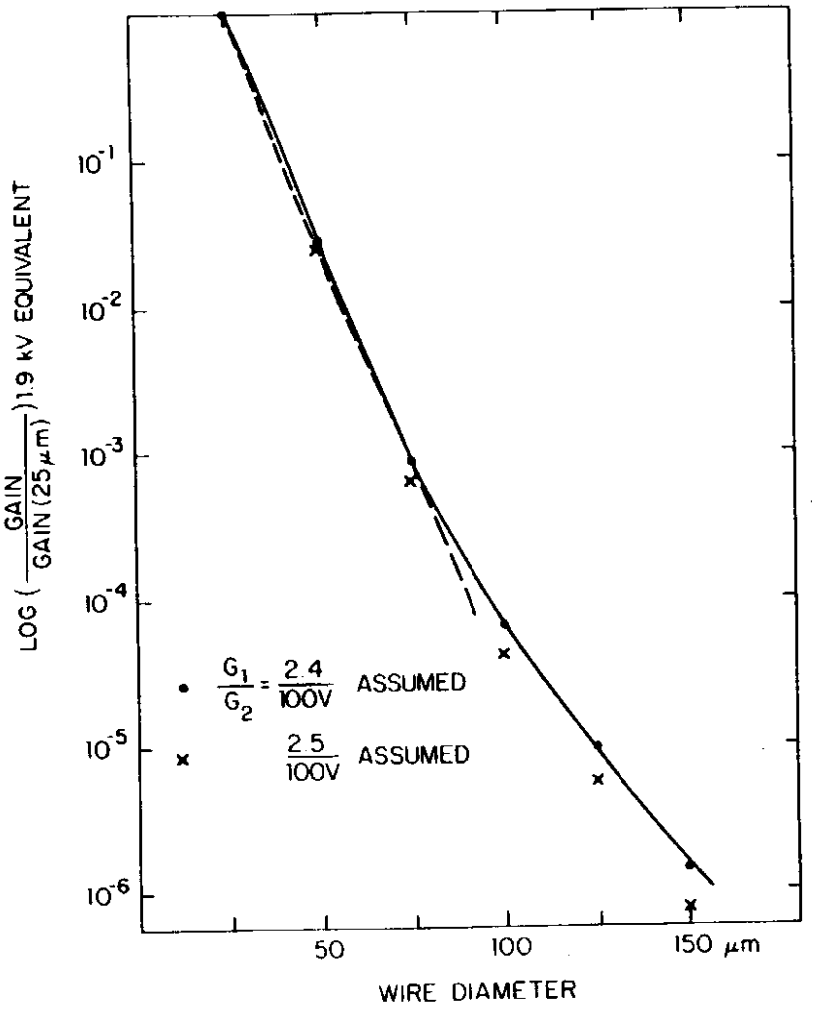
LOG (GAIN / GAIN(25 μm)) 1.9 kV EQUIVALENT
10^-1
10^-2
10^-3
10^-4
10^-5
10^-6
G1/G2 = 2.4/100V ASSUMED
2.5/100V ASSUMED
50
100
150 μm
WIRE DIAMETER

Fig. 1

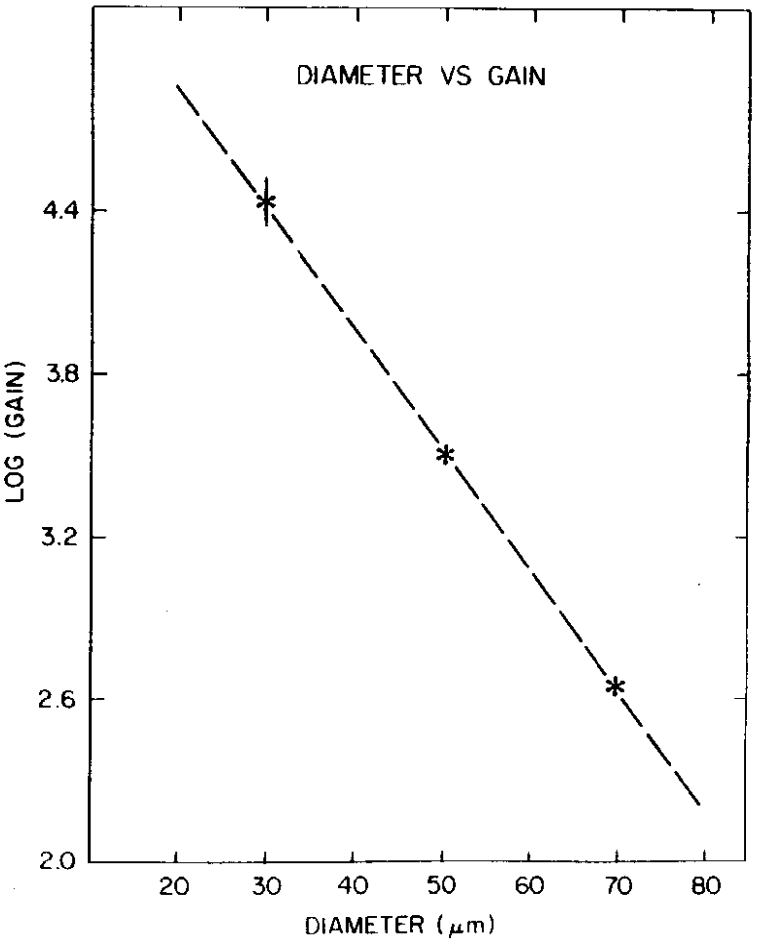
DIAMETER VS GAIN
LOG (GAIN)
4.4
3.8
3.2
2.6
2.0
20
30
40
50
60
70
80
DIAMETER (μm)

Fig. 2

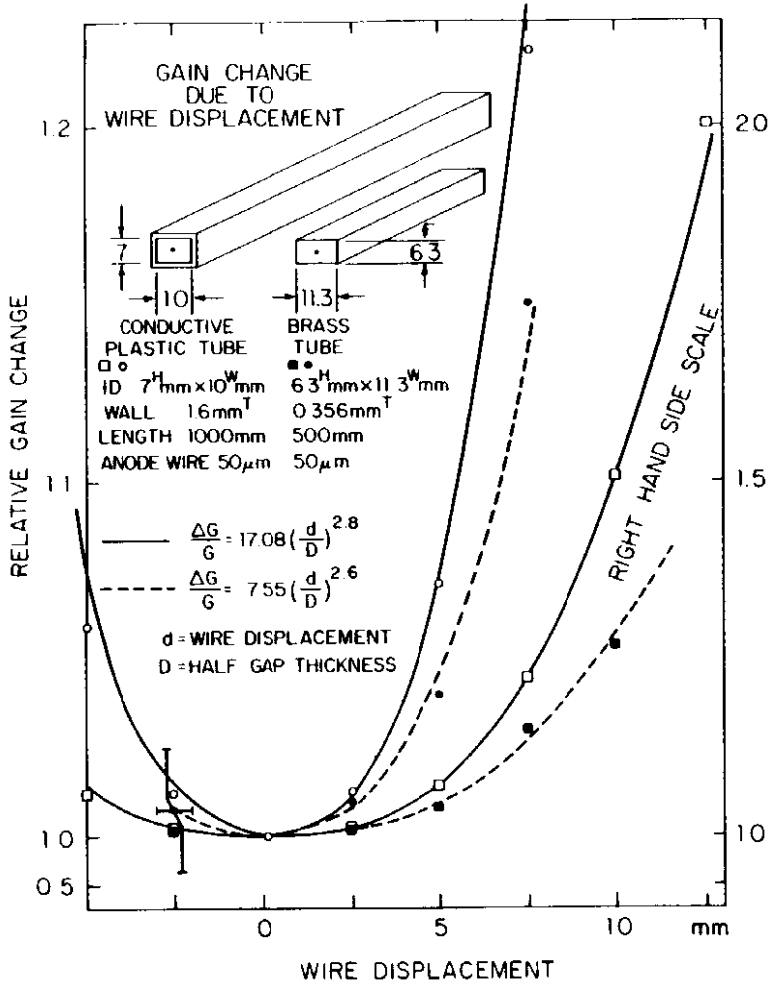
GAIN CHANGE
DUE TO
WIRE DISPLACEMENT
7
10
11.3
6.3
CONDUCTIVE
PLASTIC TUBE
BRASS
TUBE
ID 7Hmm×10Wmm
6.3Hmm×11.3Wmm
WALL 1.6mmT
0.356mmT
LENGTH 1000mm
500mm
ANODE WIRE 50μm
50μm
ΔG/G = 17.08(d/D)^2.8
ΔG/G = 7.55(d/D)^2.6
d = WIRE DISPLACEMENT
D = HALF GAP THICKNESS
RELATIVE GAIN CHANGE
RIGHT HAND SIDE SCALE
1.2
1.1
1.0
0.5
2.0
1.5
1.0
0
5
10
mm
WIRE DISPLACEMENT

Fig. 3

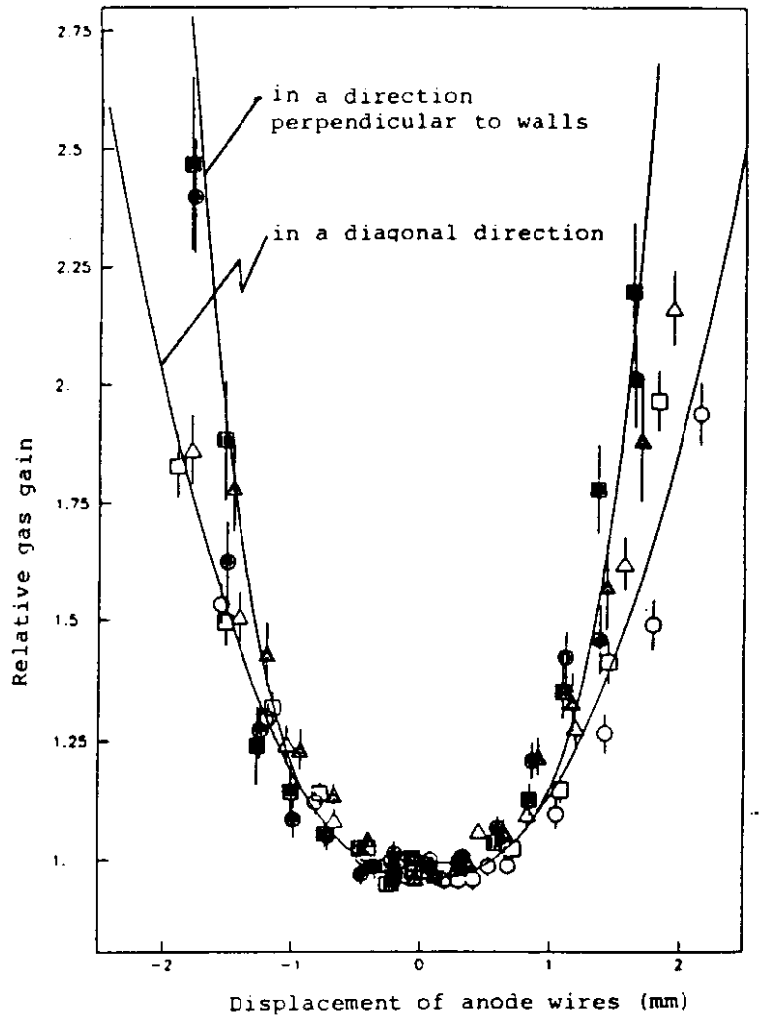
in a direction
perpendicular to walls
in a diagonal direction
Relative gas gain
2.75
2.5
2.25
2.
1.75
1.5
1.25
1.
-2
-1
0
1
2
Displacement of anode wires (mm)

Fig. 4

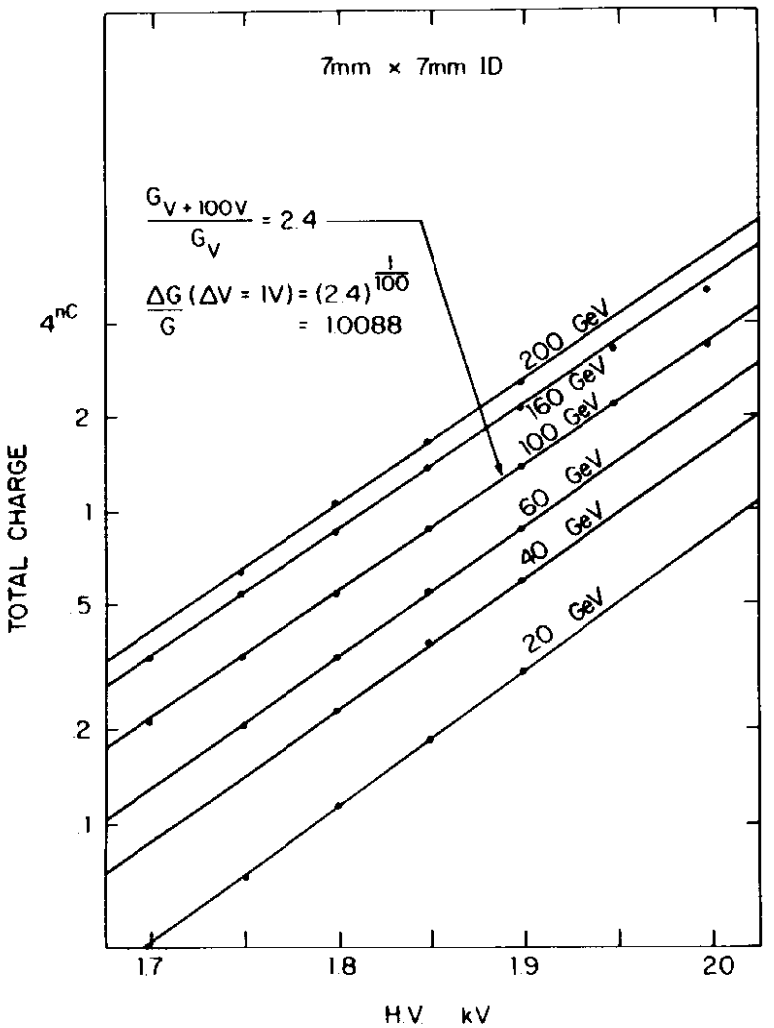
7mm × 7mm ID
$\frac{G_{V+100V}}{G_V} = 2.4$
$\frac{\Delta G}{G}(\Delta V = IV) = (2.4)^{\frac{1}{100}}$
$= 10088$
200 GeV
160 GeV
100 GeV
60 GeV
40 GeV
20 GeV
TOTAL CHARGE
4nC
2
1
5
2
1
1.7
1.8
1.9
20
H.V kV

Fig. 5

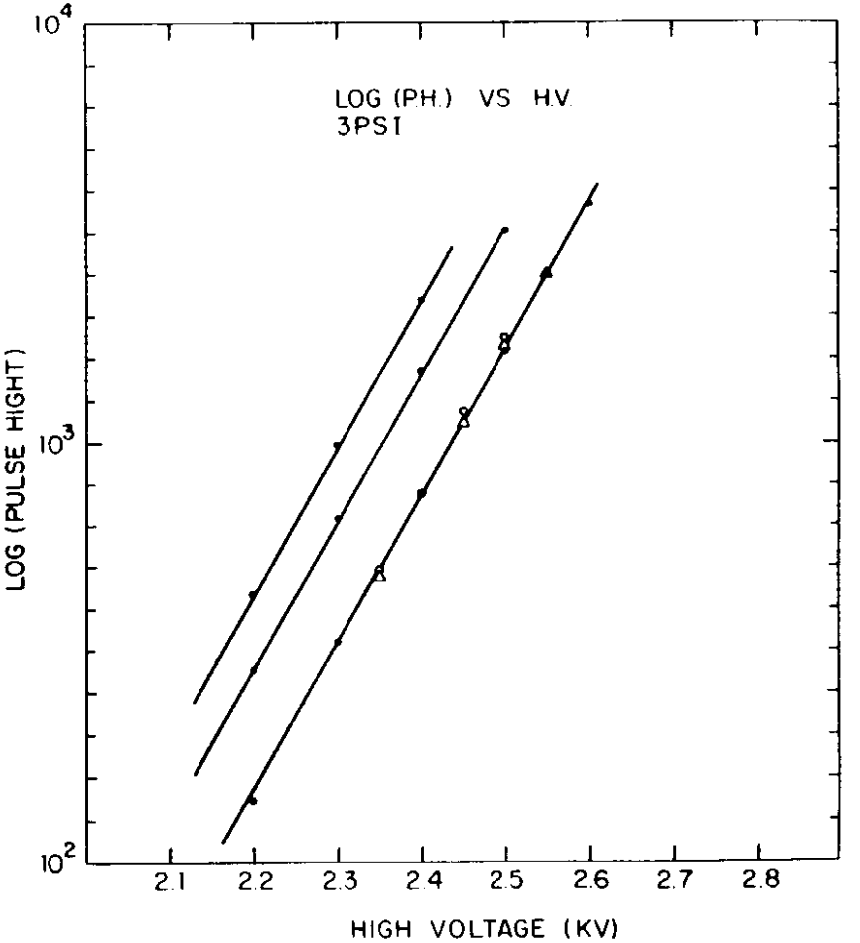
LOG (PH.) VS H.V
3PSI
LOG (PULSE HIGHT)
10^4
10^3
10^2
2.1
2.2
2.3
2.4
2.5
2.6
2.7
2.8
HIGH VOLTAGE (KV)

Fig. 6

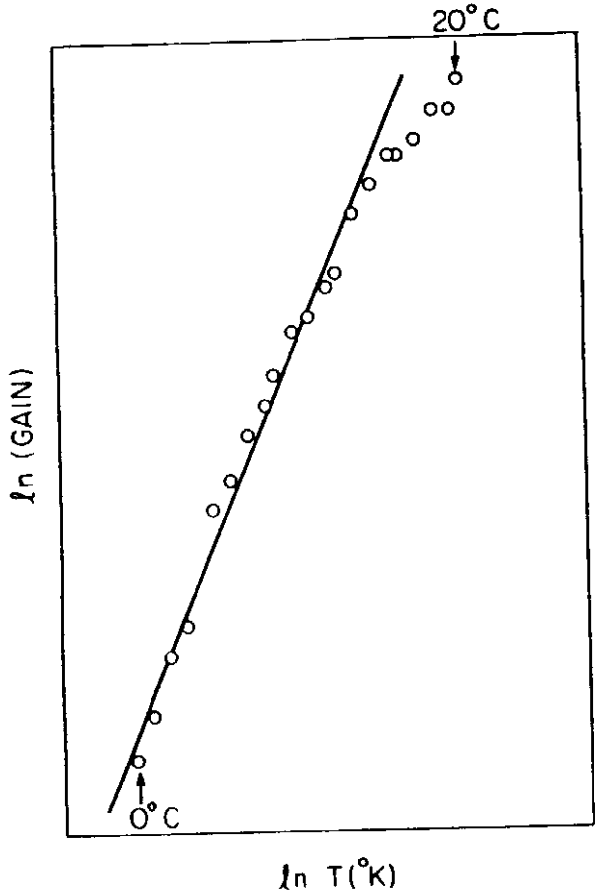

Fig. 7

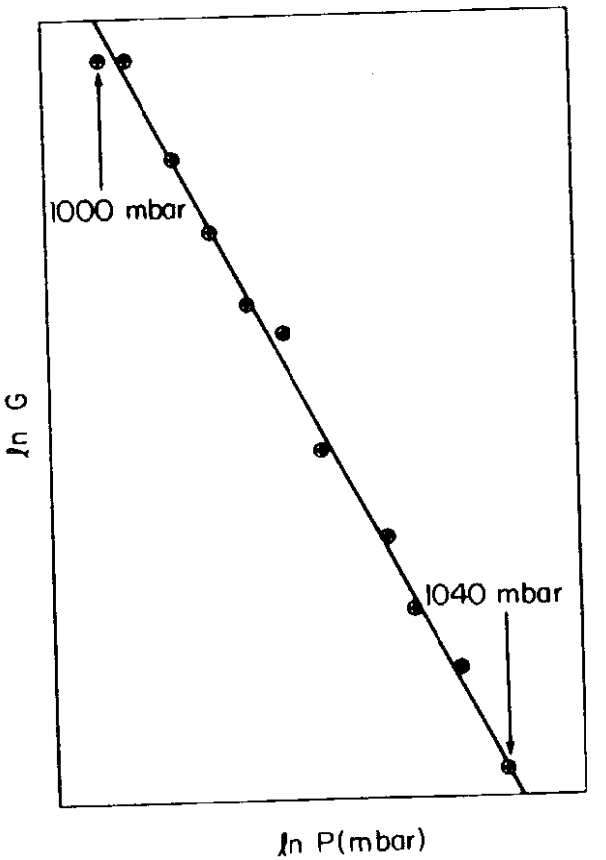

Fig. 8

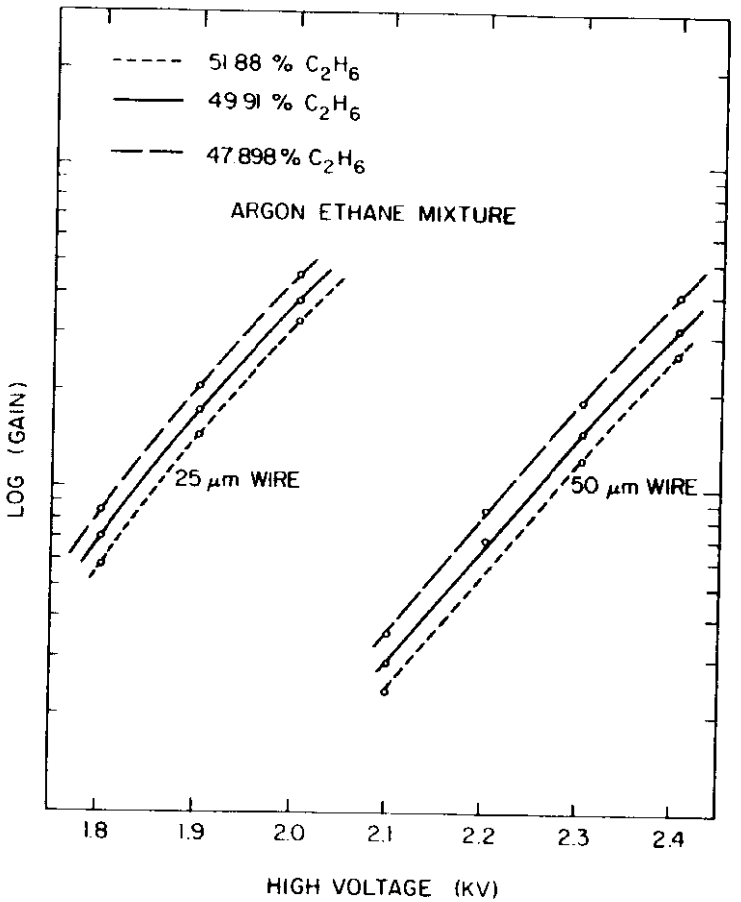
51.88 % C_2H_6
49.91 % C_2H_6
47.898 % C_2H_6
ARGON ETHANE MIXTURE
25 μm WIRE
50 μm WIRE
LOG (GAIN)
1.8
1.9
2.0
2.1
2.2
2.3
2.4
HIGH VOLTAGE (KV)

Fig. 9

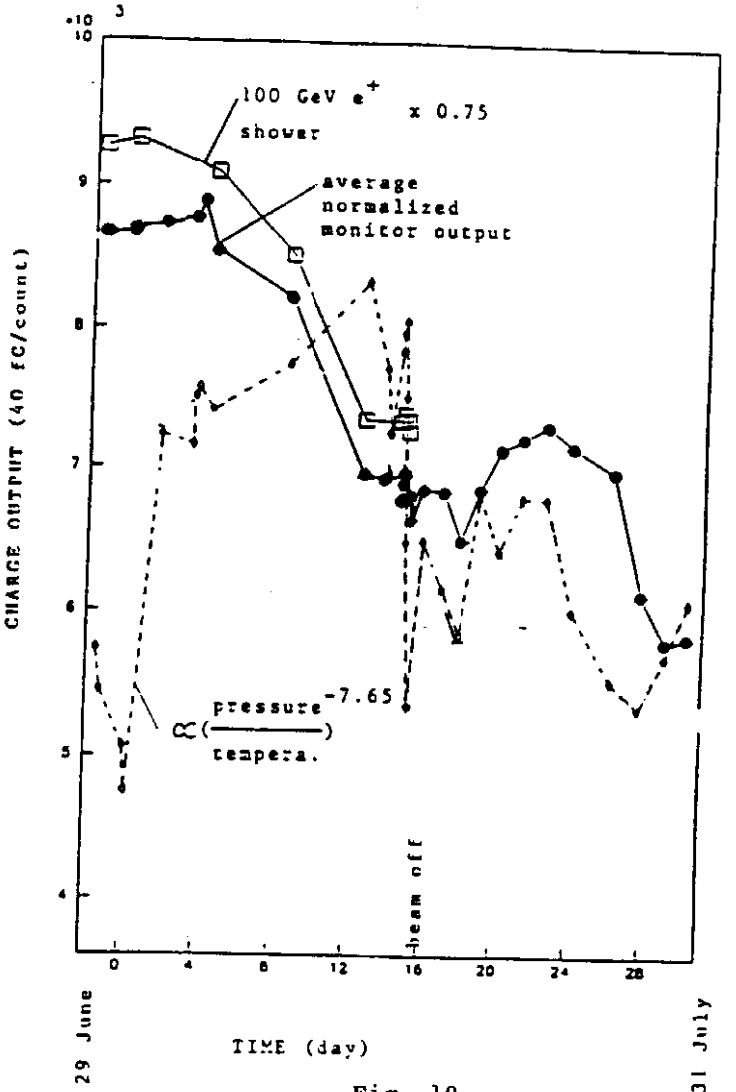
100 GeV e^+
shower
x 0.75
average
normalized
monitor output
$\propto \left(\frac{\text{pressure}}{\text{tempera.}}\right)^{-7.65}$
beam off
CHARGE OUTPUT (40 fC/count)
TIME (day)
29 June
31 July

Fig. 10